

# Effect of Temperature on Photosynthesis and Growth in Marine *Synechococcus* spp.<sup>1</sup>[C][OPEN]

Katherine R.M. Mackey\*, Adina Paytan, Ken Caldeira, Arthur R. Grossman, Dawn Moran, Matthew McIlvin, and Mak A. Saito

Bay Paul Center for Comparative Molecular Biology and Evolution, Marine Biological Laboratory, Woods Hole, Massachusetts 02543 (K.R.M.M.); Institute for Marine Science, University of California, Santa Cruz, California 95064 (K.R.M.M., A.P.); Department of Marine Chemistry and Geochemistry, Woods Hole Oceanographic Institution, Woods Hole, Massachusetts 02543 (K.R.M.M., D.M., M.M., M.A.S.); and Department of Global Ecology (K.C.), and Department of Plant Biology (A.R.G.), Carnegie Institution for Science, Stanford, California 95036

In this study, we develop a mechanistic understanding of how temperature affects growth and photosynthesis in 10 geographically and physiologically diverse strains of *Synechococcus* spp. We found that *Synechococcus* spp. are able to regulate photochemistry over a range of temperatures by using state transitions and altering the abundance of photosynthetic proteins. These strategies minimize photosystem II (PSII) photodamage by keeping the photosynthetic electron transport chain (ETC), and hence PSII reaction centers, more oxidized. At temperatures that approach the optimal growth temperature of each strain when cellular demand for reduced nicotinamide adenine dinucleotide phosphate (NADPH) is greatest, the phycobilisome (PBS) antenna associates with PSII, increasing the flux of electrons into the ETC. By contrast, under low temperature, when slow growth lowers the demand for NADPH and linear ETC declines, the PBS associates with photosystem I. This favors oxidation of PSII and potential increase in cyclic electron flow. For *Synechococcus* sp. WH8102, growth at higher temperatures led to an increase in the abundance of PBS pigment proteins, as well as higher abundance of subunits of the PSII, photosystem I, and cytochrome b6f complexes. This would allow cells to increase photosynthetic electron flux to meet the metabolic requirement for NADPH during rapid growth. These PBS-based temperature acclimation strategies may underlie the larger geographic range of this group relative to *Prochlorococcus* spp., which lack a PBS.

Marine picocyanobacteria are the most abundant phytoplankton, inhabiting nearly every area of the surface ocean and dominating in tropical and subtropical waters. The smallest and most abundant marine picocyanobacteria belong to the genera *Synechococcus* and *Prochlorococcus*, which together account for one-third of the total primary production on Earth (Partensky et al., 1999b). Marine *Synechococcus* spp. are genetically diverse (Scanlan et al., 2009; Mazard et al., 2012), play an important role in the biogeochemical cycling of carbon (Grob et al., 2007), and are found from the equator to the polar circle, though they are less abundant at higher

latitudes (Agusti, 2004; Scanlan et al., 2009; Huang et al., 2012). Temperature is a major factor that controls photosynthetic rates, and the biogeography of *Synechococcus* spp. strains in the modern ocean has been linked to temperature (Zwirgmaier et al., 2008). In this study, we explore the effect of temperature on growth and photosynthesis in several *Synechococcus* spp. strains.

Photosynthetic electron transport in cyanobacteria, including *Synechococcus* spp., shares similarities with that of plants and green algae (Fig. 1). Photosynthetic organisms are commonly able to perform photosynthesis efficiently over a range of temperatures bracketing the optimal growth temperature ( $T_{opt}$ ). However, decreased metabolic rates at temperatures too far below  $T_{opt}$  can cause an imbalance between photochemistry and metabolism, leading to photodamage (Huner et al., 1996). By contrast, elevated temperatures may affect membrane fluidity and denature proteins, which can also lead to a decline in photosynthetic efficiency (Falk et al., 1996). A range of diverse acclimation strategies have evolved among algae and plants to balance electron flow through the electron transport chain (ETC) during temperature fluctuations (Maxwell et al., 1994; Krol et al., 1997; Gray et al., 1998; Miśkiewicz et al., 2000).

Less is known about mechanisms marine cyanobacteria use to acclimate to temperature. Cyanobacteria

<sup>1</sup> This work was supported by National Science Foundation Oceanography grants (grant no. OCE-0850467 to A.P. and grant no. OCE-1220484 to M.A.S.), a grant from the Gordon and Betty Moore Foundation (grant no. GBMF-2724 to M.A.S.), and a National Science Foundation Postdoctoral Research Fellowship in Biology (grant no. NSF 1103575 to K.R.M.M.).

\* Address correspondence to kmackey@whoi.edu.

The author responsible for distribution of materials integral to the findings presented in this article in accordance with the policy described in the Instructions for Authors ([www.plantphysiol.org](http://www.plantphysiol.org)) is: Katherine R.M. Mackey (kmackey@whoi.edu).

[C] Some figures in this article are displayed in color online but in black and white in the print edition.

[OPEN] Articles can be viewed online without a subscription.

[www.plantphysiol.org/cgi/doi/10.1104/pp.113.221937](http://www.plantphysiol.org/cgi/doi/10.1104/pp.113.221937)

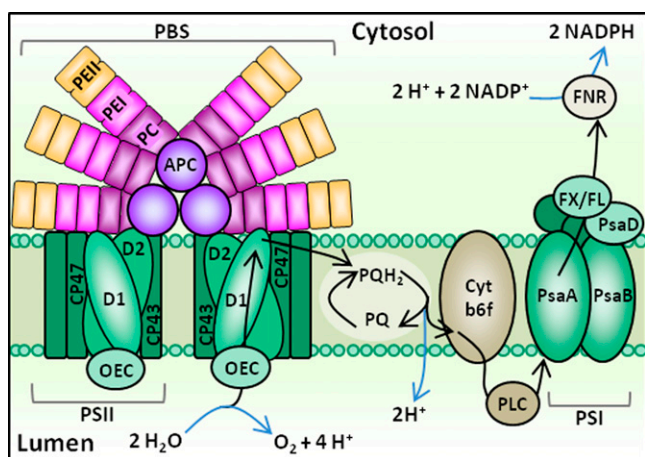


**Figure 1.** PBS structure and linear photosynthetic electron flow in cyanobacteria. In this schematic, the PBS is in “state 1,” indicating it is associated with a PSII dimer. Photosynthetic electron flow pathways are indicated by black arrows, and chemical reactions are indicated by blue arrows. Major ETC components include PSII, PSI, PQ/plastoquinone ( $PQH_2$ ), cytochrome *b6f* (Cyt *b6f*), plastocyanin (PLC), ferredoxin (FX), flavodoxin (FL), and ferredoxin/flavodoxin NADP reductase (FNR). Other proteins depicted include the phycobiliproteins APC, PC, two forms of PE (PE I and PE II), PSII chlorophyll-binding proteins CP47 and CP43, the PSII core polypeptides D1 and D2, the PSI chlorophyll-binding core proteins PsaA and PsaB, and the PSI reaction center subunit PsaD. [See online article for color version of this figure.]

differ from plants and green algae in that photosynthesis and respiration occur in the same membrane. In addition, the ratios of PSII:PSI are more variable in cyanobacteria (Campbell et al., 1998; Bailey et al., 2008), which can impact the flow of electrons through the ETC. Cells must prevent overreduction of the ETC because this can lead to damage of the D1 polypeptide of PSII in a process called photoinhibition; to sustain PSII activity, replacement of the damaged D1 by de novo protein synthesis is required (Aro et al., 1993). Cyanobacteria have evolved a suite of strategies to balance electron flow in the thylakoid membrane when the cells are exposed to high light; important strategies include nonphotochemical quenching (El Bissati et al., 2000; Bailey and Grossman, 2008) and alternative electron flow pathways (Asada, 1999; Bailey et al., 2008; Mackey et al., 2008). Cyanobacteria may also selectively funnel light energy to PSII or PSI to regulate the amount of electrons entering and exiting the ETC (Campbell et al., 1998).

In cyanobacteria, including *Synechococcus* spp., the main light-harvesting antennae are water-soluble pigment-protein complexes called phycobilisomes (PBSs; Grossman et al., 1993; Six et al., 2007). Unlike the antenna of plants and algae that are embedded within the thylakoid membrane, PBSs are located on the cytoplasmic surface of the membrane (Fig. 1). Structurally, the PBS consists of phycobiliproteins, including the PBS core allophycocyanin (APC) and lateral rods of phycocyanin (PC) and phycoerythrin (PE; Fig. 1). The PBS core has

evolved together with the core genome of *Synechococcus* spp., whereas the rod components appear to have evolved separately through gene duplication, DNA exchange between cells, and possibly virally mediated lateral gene transfer (Six et al., 2007). Each phycobiliprotein binds chromophores called phycobilins (linear tetrapyrroles) that selectively absorb different wavelengths of green-red light, thereby extending the range of photosynthetically active radiation the cell can use beyond that of chlorophyll (Campbell et al., 1998). The PBS is capable of rapid diffusion over the thylakoid membrane surface (Mullineaux et al., 1997), where it can associate with either PSI or PSII. The PBS is a mobile antenna element that does not bind chlorophyll and that likely associates with reaction centers by weak interactions with lipid head groups (Sarcina et al., 2001).

State transitions, the movements of PBS or other antenna pigments between reaction centers, allow the cells to avoid PSII photodamage by balancing electron flow such that electrons do not accumulate within the ETC. Whether the PBS associates with PSI or PSII is determined by the redox poise of the plastoquinone (PQ) pool (Fig. 1), which serves as an indicator of electron flow through the ETC. When the PQ pool is oxidized, the PBS becomes associated with PSII (state 1) such that the rate of linear electron flow increases. By contrast, a reduced PQ pool elicits affiliation of the PBS with PSI (state 2), which could increase the withdrawal of electrons from the ETC. In the dark, the PQ pool tends to be reduced due to respiratory electron flow, and the PBS affiliates primarily with PSI.

Recent ocean basin scale research has shed light on the role of temperature on the global distributions of *Synechococcus* spp. in the ocean. Collectively, these studies have shown that marine *Synechococcus* spp. tolerate a broad range of temperatures, likely due to high genetic diversity among strains. For example, of the four clades that dominate in natural communities, clades I and IV typically inhabit cooler waters north of 30°N and south of 30°S (Brown et al., 2005; Zwirgmaier et al., 2007, 2008), while clades II and III generally inhabit warmer tropical and subtropical waters (Fuller et al., 2006; Zwirgmaier et al., 2008). Other *Synechococcus* spp. sequences have been recently identified from colder waters in the northern Bering Sea and Chukchi Sea, suggesting that a possible cold adaptation could exist in some strains present at high latitudes (Huang et al., 2012). Still, other studies have found no relationship between *Synechococcus* spp. abundance and temperature (Zinser et al., 2007), suggesting that additional factors (e.g. nutrient availability) may be responsible for shaping *Synechococcus* spp. community structure (Palenik et al., 2003, 2006; Scanlan et al., 2009).

While field surveys have made great strides in understanding the role of temperature in controlling picocyanobacteria distributions, much remains to be learned about the range of growth responses to temperature that can occur in marine *Synechococcus* spp. To date, characterization of individual *Synechococcus*

spp. strains includes work with two isolates from the Sargasso Sea, showing variable responses to temperature (Moore et al., 1995; Fu et al., 2007). These studies demonstrate the potential for changing sea surface temperature (SST) to influence the biogeochemical role of *Synechococcus* spp. in the Sargasso Sea; however, little is known about whether these responses can be generalized to other strains or environments. Changes in growth rate and photosynthetic efficiency, if they occur, could alter global *Synechococcus* spp. distributions, affect ecosystem structure, and ultimately impact marine biogeochemical cycles and Earth's climate, and thus could have important implications for the earth system.

A mechanistic understanding of how temperature affects growth and photosynthesis in geographically and physiologically diverse strains of *Synechococcus* spp. is needed to clarify how temperature influences *Synechococcus* spp. biogeography, as well as to provide insights into how populations are likely to respond to increased SST in the future. The goal of this study is to characterize the growth, photosynthetic efficiency, and light-harvesting characteristics of 10 diverse *Synechococcus* spp. isolates over a range of temperatures. Using chlorophyll fluorescence analysis, we show that regulation of light harvesting via state transitions is an important acclimation process that allows cells to increase photosynthetic electron flow under high temperature conditions. This effect is enhanced for strains with higher proportions of phycoerythrobilin and phycourobilin. We use global proteome data from *Synechococcus* sp. WH8102 to show that this temperature-dependent enhancement is brought about in part by an increase in the abundance of PBS proteins, as well as proteins from PSII, PSI, and other ETC components. The results are discussed in the context of *Synechococcus* spp. biogeography in the modern ocean, and potential implications for how cells could respond to future increases in SST are considered.

## RESULTS

Experiments were conducted using two strains of *Synechococcus* spp. isolated from throughout the world's

oceans (Fig. 2). Fluorescence traces were collected using pulse amplitude-modulated (PAM) fluorometry as described in "Materials and Methods," and photosynthetic parameters were derived from these traces (Fig. 3).

### SST Measurements

Seasonal SST variations were evident at the site of origin for each strain, with the largest temperature fluctuations occurring at higher latitudes. The smallest fluctuation in temperature occurred at equatorial sites, where strains CCMP1183 and CCMP1379 (Fig. 4; Table I) were collected. The site with the largest seasonal SST variation was Beifang Bay, where strain CCMP1632 was isolated and where the SST ranged from 3.2°C to 24.6°C over the course of the year.

### Growth and Photophysiology

#### *Doubling Time and Maximum Photochemical Efficiency*

The growth and photosynthetic responses of each of the strains to changes in temperature are presented in Figure 5, and the optimal temperatures for each parameter are given in Table I. For four of the strains (CCMP1379, CCMP1630, CCMP2606, and PCC 7002) growth rate continued to increase up to 27°C without reaching a plateau, indicating that maximum growth rate temperatures for these strains were above 27°C. The values of photochemical efficiency of PSII in the dark-adapted state ( $F_v/F_m$ ) for these strains remained at or near maximal levels at 27°C. For the remaining strains, maximal growth rates were observed at lower temperatures within the range we tested, and  $F_v/F_m$  values were highest within  $\pm 6^\circ\text{C}$  of the maximum growth temperature. Overall, while the growth rate exhibited an incremental response to changing temperature,  $F_v/F_m$  showed more of a threshold response, increasing sharply once a critical temperature was reached and maintaining relatively stable values for all temperatures when the cells were actively dividing. High maximum photosynthetic efficiency appears to

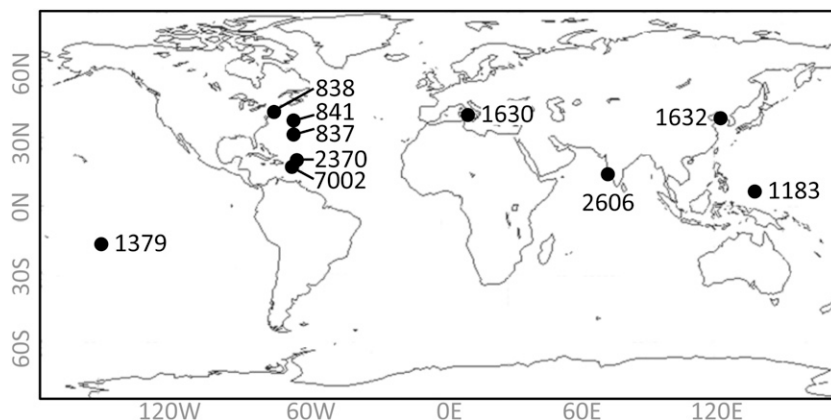


**Figure 2.** Map of strain origins. Exact latitude and longitude are given in Table I. (CCMP2370 and WH8102 are strain synonyms.)

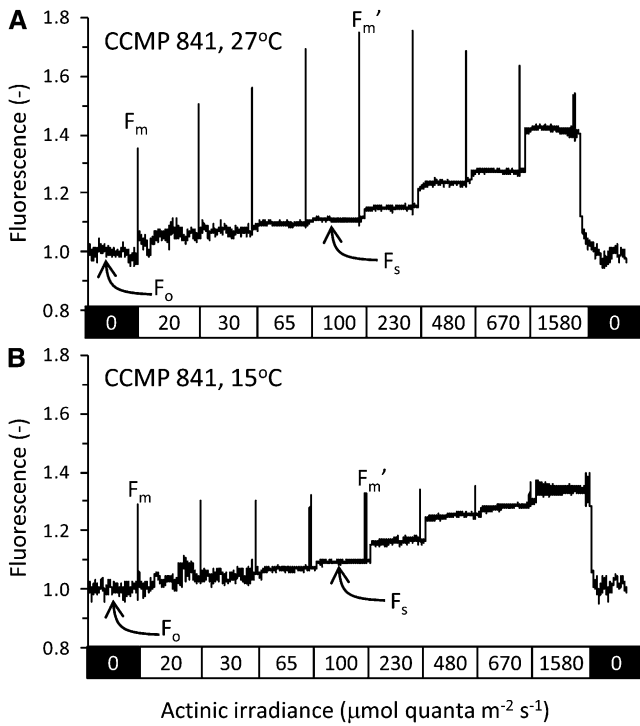


**Figure 3.** Example fluorescence traces showing PSII fluorescence for strain CCMP841 at 27°C (A) and 15°C (B). Actinic irradiances are indicated in the rectangles below each trace, and exposure to each irradiance lasted 60 s. A saturating pulse 800 ms in duration was used to temporarily close all PSII reaction centers and eliminate photochemical quenching such that maximum fluorescence levels at each irradiance could be determined. The dark-adapted steady-state fluorescence ( $F_o$ ), the fluorescence level following a saturating flash in the dark with no actinic light ( $F_m$ ), the steady state fluorescence at a given actinic intensity ( $F_s$ ), and the fluorescence level following a saturating flash in the presence of background actinic light ( $F_m'$ ) are also labeled. Each actinic irradiance level has its own unique value of  $F_s$  and  $F_m'$ , but only the values for the actinic irradiance level of 100  $\mu\text{mol quanta m}^{-2} \text{s}^{-1}$  are labeled in the figure. A strong state transition is apparent at 27°C for this strain at all actinic irradiances and can be identified from the higher  $F_m'$  values as compared with the  $F_m$  value. This indicates movement of the PBS from PSI in the dark to PSII in the light, causing increased PSII fluorescence. The effect is much less pronounced for cells grown at 15°C, where  $F_m$  and  $F_m'$  levels are more similar.

occur over a broader range of temperatures than high cell division rates.

**Photosynthetic Efficiency under Increasing Irradiance**

The photosynthetic efficiency,  $\Phi_{\text{PSII}}$  of each strain was assessed over a range of irradiances at each growth temperature (Fig. 6). Photosynthetic yields remained high for irradiances up to 230  $\mu\text{mol quanta m}^{-2} \text{s}^{-1}$ ; above 230  $\mu\text{mol quanta m}^{-2} \text{s}^{-1}$ , the yield decreased for all strains. Yields at the highest irradiance of 1,580  $\mu\text{mol quanta m}^{-2} \text{s}^{-1}$  were strongly depressed and approached zero, indicating that many PSII reaction centers were closed by this high light treatment.

However, for some strains and temperatures, the yield was not completely depressed at 1,580  $\mu\text{mol quanta m}^{-2} \text{s}^{-1}$ . For example, strains 837 and 2370 retained approximately 40% of their photosynthetic efficiency at 1,580  $\mu\text{mol quanta m}^{-2} \text{s}^{-1}$  relative to the  $F_v/F_m$  values.

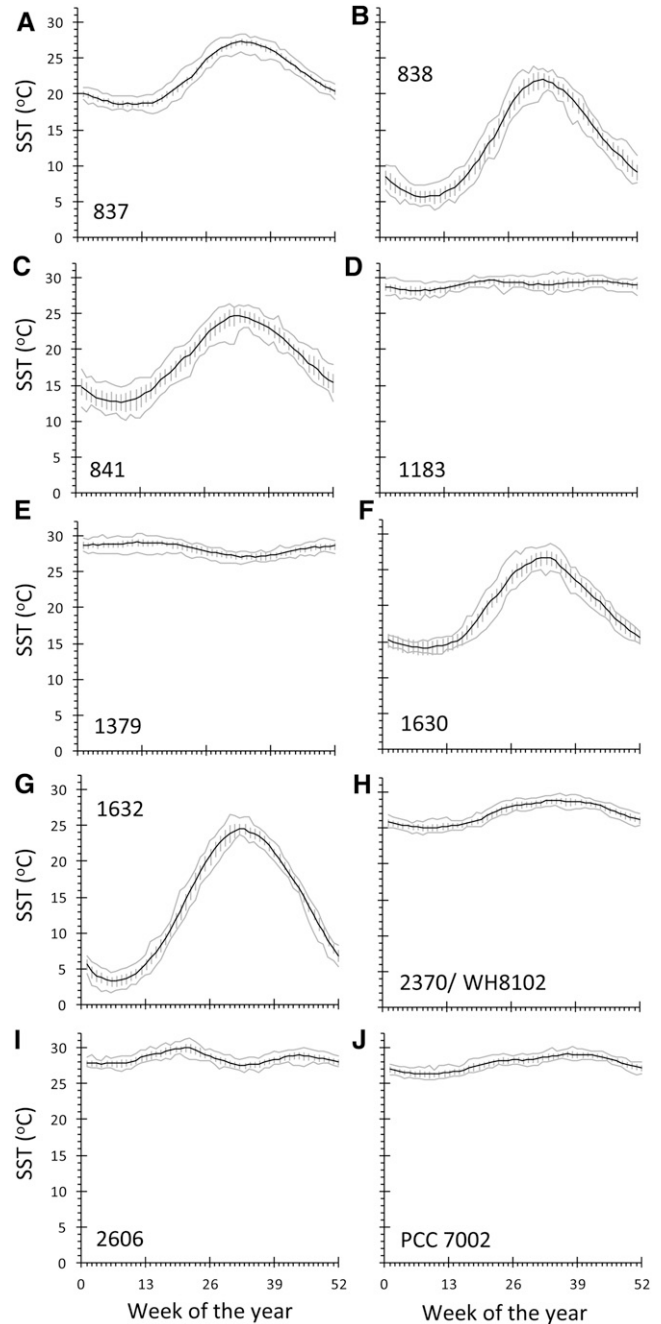


**Figure 4.** Annual cycle of SST for each strain's site of origin. The black line shows average temperature for each week, gray lines show minimum and maximum values for each week over the entire period of record, and error bars show SD for weekly mean SST values over the period January 1990 to December 2011.

**Table 1.** *Synechococcus* spp. strain origins and temperature preferences

Strain	Location and Date of Isolation	Pigment Type <sup>a</sup>	Minimum Annual Temperature <sup>b</sup>	Maximum Annual Temperature <sup>b</sup>	Average Annual Temperature <sup>b</sup>	Approximate Temperature at Time of Isolation <sup>b</sup>	Maximum Growth Rate Temperature <sup>c</sup>	Maximum $F_v/F_m$ Temperature <sup>c</sup>
			(°C)	(°C)	(°C)	(°C)	(°C)	(°C)
WH7805 (CCMP837)	33.7413°N, 67.5°W; Sargasso Sea, North Atlantic; June 30, 1978	2	21.7	28.7	22.5	26	18–24	21 ± 1.5
CCMP1183	7.5°N, 134.5°E; near Palau, North Pacific; March 1, 1983	1	28.3	29.7	29.1	28	24 ± 1.5	18 ± 1.5
CCMP1379	14.87°S, 148.68°W; Mataiva, near Tahiti, Society Islands, South Pacific; surface; 1985	1	27.1	29.2	28.3	Unknown	≥27	21 ± 1.5
CCMP1630	40.75°N, 13.90°E; Ischia, Italy, near an offshore hot spring; Mediterranean, Tyrrhenian Sea; October 5, 1985	1	14.1	26.7	19.6	22 (or higher due to hot spring influence)	≥27	21 ± 1.5
CCMP1632	38.6°N, 118.65°E (approximately); Tiansin, China (Wuhan), Beifang harbor, East China Sea, North Pacific; June 3, 1985	1	3.2	24.6	13.6	17	21 ± 1.5	21 ± 1.5
WH8102 (CCMP2370)	22.495°N, 65.6°W; Sargasso Sea, North Atlantic, from Oceanus cruise 92; March 15, 1981	3c	25.1	28.9	27.0	25	21 ± 1.5	24 ± 1.5
CCMP2606	15.31°N, 72.59°E; Arabian Sea, Indian Ocean near Goa, India; surface; October 2004	1	27.6	30.1	28.6	28	≥27	21 ± 1.5
PCC 7002	17.969809°N, 67.046052°W; onshore, marine mud sample derived from fish pens on Magueyes Island, La Parguera, Puerto Rico; Caribbean Sea, North Atlantic; 1961	1	26.3	29.2	27.8	Unknown	≥27	21 ± 1.5
WH8018 (CCMP838)	41.5250°N, 70.6736°W; Woods Hole, Massachusetts; North Atlantic; June 1980	2	5.6	22.0	13.0	16	ND	ND
CCMP841	39.5°N, 66.5°W (approximately); Research vessel Cape Hatteras Cruise, Gulf of Maine to North Atlantic; open ocean; August 1980	2	12.7	24.8	18.4	26	ND	ND

<sup>a</sup>Pigment types are described by Six et al. (2007). <sup>b</sup>SST values were based on the weekly mean SST values over the period January 1990 to December 2011 as shown in Figure 4. The average annual temperature is the mean of all weekly values throughout the year. Minimum and maximum values are the lowest and highest weekly averaged temperature, as indicated by the ranges of the black lines in Figure 4. The approximate temperature at time of isolation is estimated to the nearest degree Celsius from the average weekly mean temperatures based on the date of isolation. "Unknown" indicates the date (and therefore temperature) of isolation is unavailable. <sup>c</sup>Optimal temperatures for growth rate and  $F_v/F_m$  were determined based on data plotted in Figure 5. Because experiments were carried out in 3°C increments, the error associated with each estimate is ±1.5°C. Strains CCMP838 and CCMP841 were only cultured at 15°C and 27°C, so  $T_{opt}$  values were not determined (ND) for these strains.

### State Transition

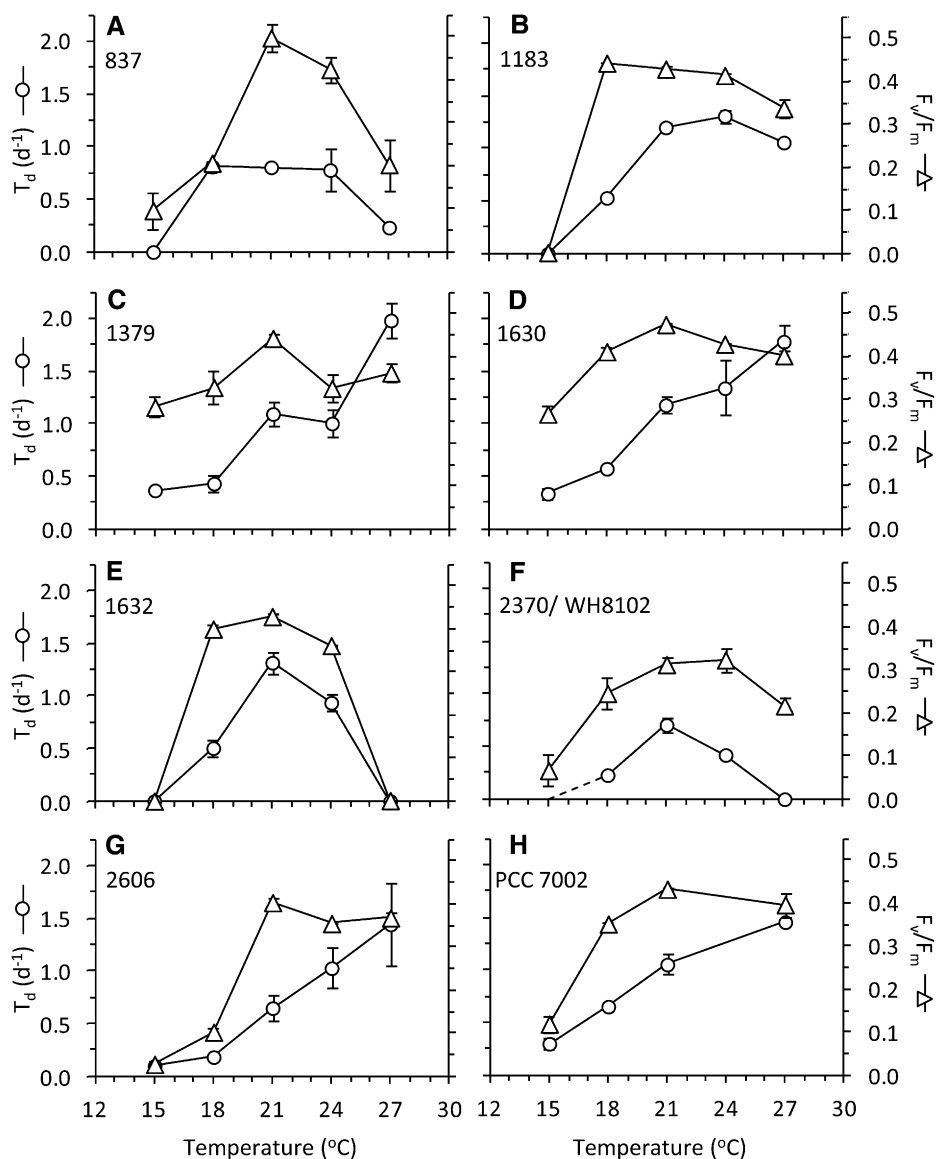
A transition of the dark-adapted cells to state 1 was observed following their exposure to actinic light. These state transitions are apparent from the light-dependent increase in maximum PSII fluorescence in the light-adapted state ( $F_m'$ ) relative to the value of maximum PSII fluorescence in the dark-adapted state ( $F_m$ ; Fig. 3), generally leading to  $\Phi_{PSII} > F_v/F_m$ . Strains with higher PE content (pink/orange strains, pigment types 2 and 3; Table I) tended to have the most pronounced transition to state 1, with the largest effect observed at 100  $\mu\text{mol quanta m}^{-2} \text{s}^{-1}$  (Fig. 3). To determine how the state transition was affected by temperature, we compared the percentage change in photosynthetic yield between 0 and 100  $\mu\text{mol quanta}$

$\text{m}^{-2} \text{s}^{-1}$  for each strain under each growth temperature as follows:

$$x\% = \frac{\Phi_{PSII-100} - (F_v/F_m)}{(F_v/F_m)} * 100$$

where  $\Phi_{PSII-100}$  is the value of  $\Phi_{PSII}$  measured with 100  $\mu\text{mol quanta m}^{-2} \text{s}^{-1}$  background light. The change in yield is a consequence of the cumulative effect of the various processes that impact fluorescence, including the transition to state 1 (which serves to increase  $\Phi_{PSII}$  relative to  $F_v/F_m$ ), as well as changes in other photochemical and nonphotochemical quenching processes.

**Figure 5.** Growth and photosynthesis of strains over a range of growth temperatures. The number of doublings per day ( $T_d$ , white circles) is plotted on the left axes, and the dark-adapted photochemical yield ( $F_v/F_m$ , white triangles) is plotted on the right axes. Error bars show SE. WH8102 grew very slowly at 15°C, approaching the limit of its temperature range under our conditions. The uncertainty in growth rate is indicated by the dashed line in panel F.



Two trends are immediately apparent from these calculations. First,  $\Phi_{\text{PSII-100}}$  is less depressed relative to  $F_v/F_m$  at higher temperatures for all strains (Fig. 7), regardless of the  $T_{\text{opt}}$  of the strain as determined by doubling time or  $F_v/F_m$  (Fig. 5; Table I). This indicates that at higher temperatures, cells are able to maintain more oxidized PSII reaction centers in the light. Second, strong transitions to state 1 are evident, where the percentage change in photosynthetic yield becomes positive, indicating  $\Phi_{\text{PSII-100}} > F_v/F_m$  (e.g. strains CCMP837, CCMP1632, CCMP2370, and CCMP2606). This indicates that more of the PBS antenna is associated with PSII reaction centers at 100  $\mu\text{mol quanta m}^{-2} \text{s}^{-1}$  than in the dark (mobile antennae move from PS1 to PSII). Because the strongest transitions to state 1 were apparent in strains with higher PE content (CCMP837 and CCMP2370), we tested two additional high PE strains (strains CCMP838 and CCMP841) at 15°C and 27°C to determine if the trend was conserved.

These pink strains showed a strong transition to state 1 (Fig. 3; Fig. 6, B and C) and higher  $\Phi_{\text{PSII-100}}$  relative to  $F_v/F_m$  at 27°C than at 15°C (Fig. 7, B and C).

#### Proteomics of CCMP2370 (WH8102)

Proteins involved in light harvesting and photosynthesis were identified from the global proteome of *Synechococcus* sp. WH8102 grown under different temperature conditions (Figs. 8 and 9). These proteins were organized into five groups based on their location in the photosynthetic apparatus, including PSI, PSII, cytochrome b6f, ferredoxin, and pigments/PBS. Figure 8 shows the relative abundance of each peptide relative to the centered mean value (see “Materials and Methods”), and Figure 9 shows the mean of normalized abundances for each group. PSI, PSII, and cytochrome b6f proteins became more abundant at 18°C

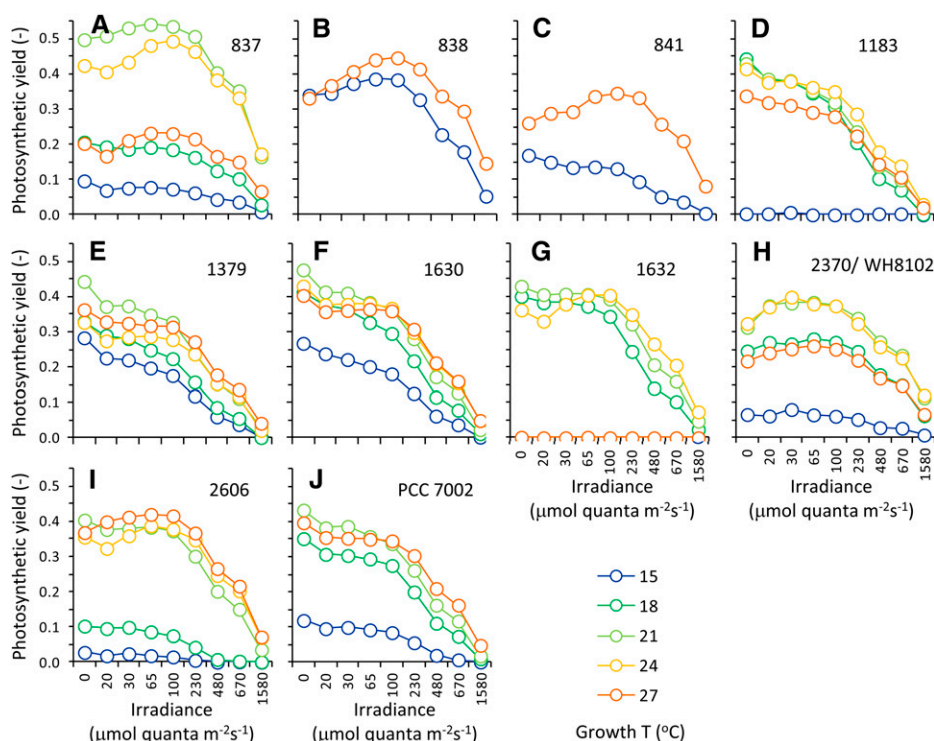


**Figure 6.** Photosynthetic yields ( $F_v/F_m$  and  $\Phi_{PSII}$ ) versus irradiance for strains grown over a range of temperatures. Legend is shown at lower right. Strains CCMP838 and CCMP841 were only cultured at 15°C and 27°C.

and 23°C than at 15°C (Figs. 8 and 9). Peptides affiliated with ferredoxin generally decreased with increasing temperature, with the exception of those involved in carbon and nitrogen metabolism, such as ferredoxin-NADP reductase, ferredoxin-dependent Glu synthase, and ferredoxin-nitrite reductase, which increased with

increasing temperature (Fig. 8). Responses of PBS-related proteins were more variable (Fig. 8), but, in general, their relative abundance increased with increasing temperature (Fig. 9). The responses of other proteins in the *Synechococcus* sp. WH8102 proteome during this study are described elsewhere (M.A. Saito, unpublished data).

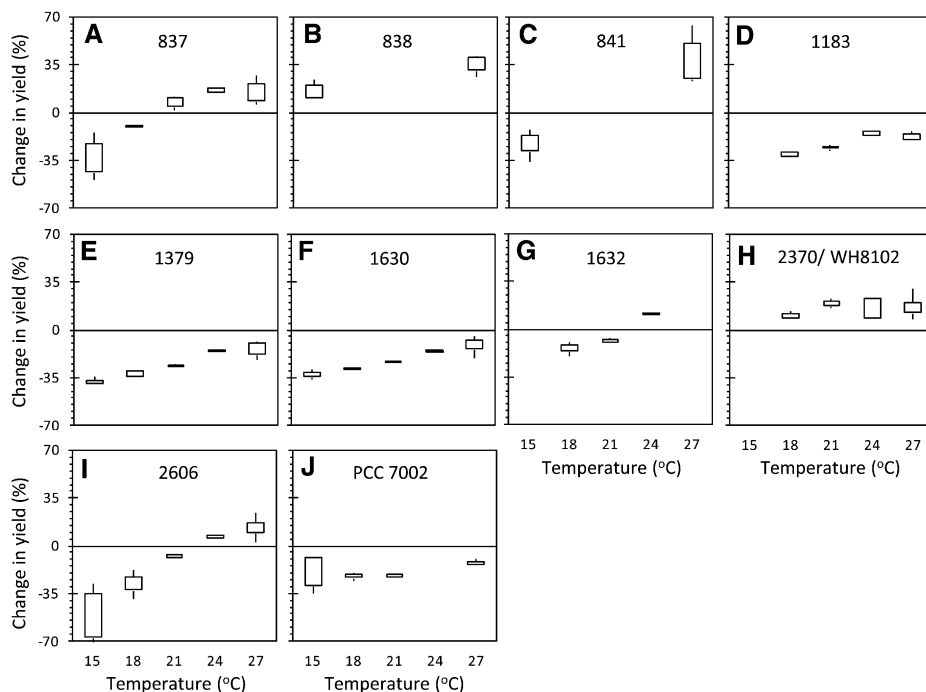


**Figure 7.** State transitions increase with temperature. Data show the percentage change in yield measured during exposure to 100  $\mu\text{mol quanta m}^{-2}\text{s}^{-1}$  background light ( $\Phi_{PSII-100}$ ) compared with yield measured in the dark ( $F_v/F_m$ ). More positive values indicate the yield increased following exposure to light relative to the dark-adapted condition. Strains 838 and 841 were only cultured at 15°C and 27°C, and strain PCC 7002 was not cultured at 24°C. Missing boxes in other plots indicate that strains did not grow at that temperature (e.g. CCMP1632 at 15°C and 27°C) or that the average of photosynthetic yields was too low to calculate meaningful percentage changes (e.g. WH8102 at 15°C).

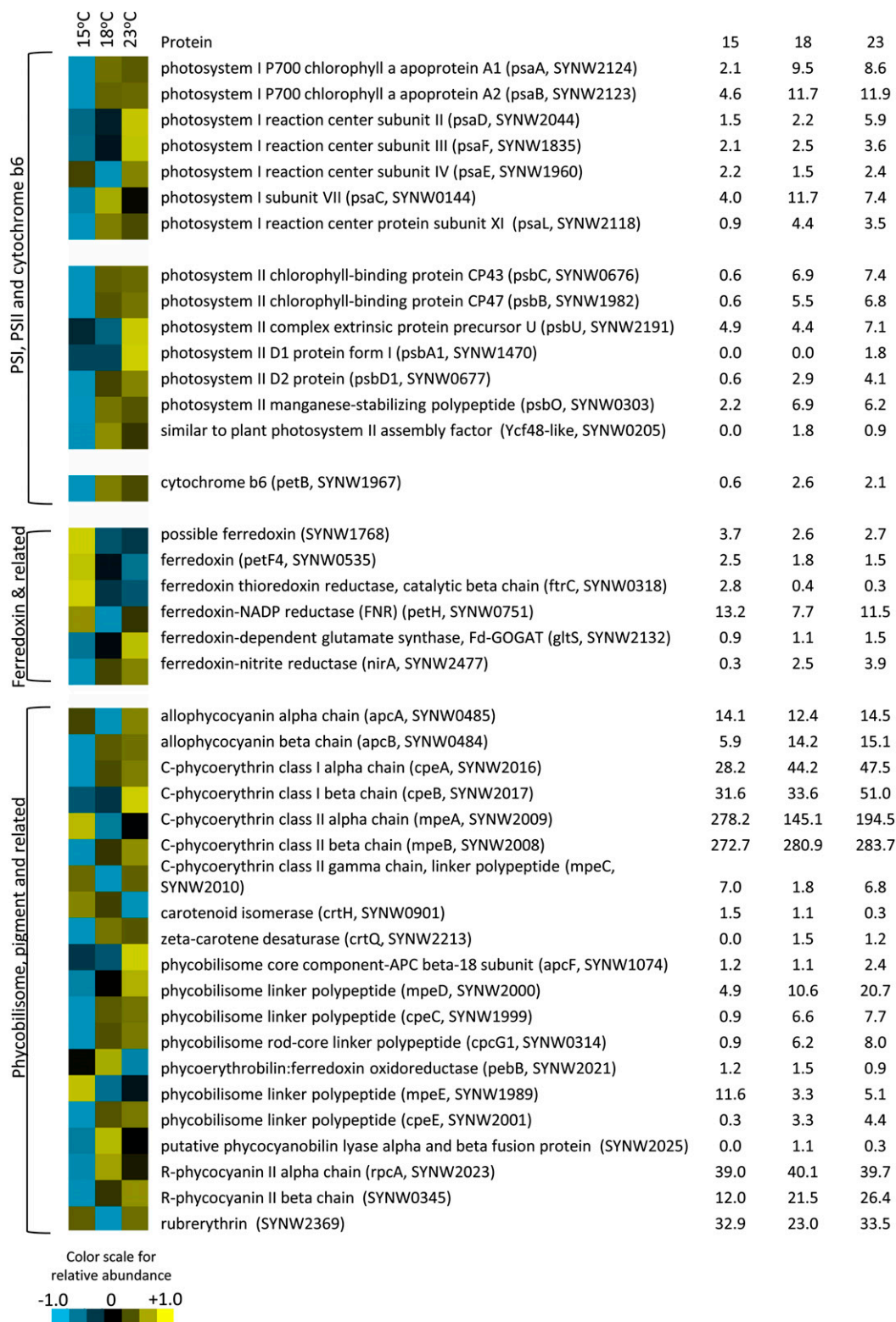


**Figure 8.** Cluster analysis of photosynthetic proteins from the *Synechococcus* sp. WH8102 (CCMP2370) global proteome at 15°C, 18°C, and 23°C. Color indicates higher (yellow) or lower (blue) relative abundance relative to the centered mean value (black). Raw spectral counts are shown at right.

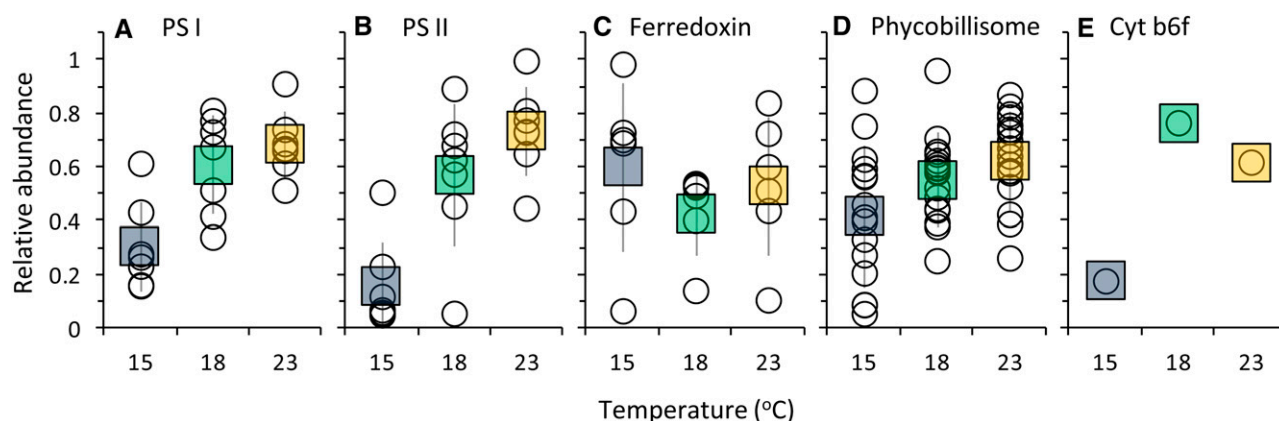


**Figure 9.** Normalized relative abundance of photosynthetic proteins in the *Synechococcus* sp. WH8102 (CCMP2370) global proteome grouped by location in the photosynthetic apparatus, including PSI (A), PSII (B), ferredoxin (and associated proteins; C), PBS (D), and cytochrome b6f (E). White circles show the relative abundances of individual peptides as indicated in Figure 8, squares show the mean for each temperature, and error bars show  $sd$  (except for cytochrome b6f, where only one peptide was identified). [See online article for color version of this figure.]

## DISCUSSION

All photosynthetic organisms face the challenge of balancing photosynthetic electron flow with the energetic demands of cell growth. Achieving balanced electron flow is critical for avoiding photoinhibition, which necessitates energetically expensive protein repair. In this study, we found that active regulation of the state transition together with changes in the abundance of photosynthetic proteins are both important mechanisms for balancing photosynthesis and growth in marine *Synechococcus* spp. over a range of temperatures.

### Photophysiology

Certain photosynthetic characteristics were shared among the 10 strains of marine *Synechococcus* spp. examined in this study. For example, photosynthetic efficiency ( $F_v/F_m$ ) for all strains is high over a range of temperatures encompassing the  $T_{opt}$  for each strain.  $F_v/F_m$  remains relatively stable for all strains over all temperatures where active growth is occurring, and only when the growth rate declines sharply is a decline in  $F_v/F_m$  observed (Fig. 5). In general, the  $F_v/F_m$  begins to increase and reaches near maximal values at lower temperatures compared with growth rate. The high efficiency of photosynthesis over all temperatures where cells are actively growing suggests that photosynthetic electron flow does not limit growth and that PSII reaction centers do not experience high excitation pressure while cells are actively growing. The metabolic demands of the cell change as growth rate responds to temperature; more reductant is required by fast-growing cells than for cells that divide slowly. The stability of  $F_v/F_m$  with temperature suggests that regulation of light harvesting and photosynthetic electron flow must coordinate with fluctuations in metabolic

demand, providing more electron flow when growth is rapid and less when growth is slow.

In nature, *Synechococcus* spp. cells must cope with a broad range of light levels that can reach up to  $2,000 \mu\text{mol quanta m}^{-2} \text{s}^{-1}$  in clear surface waters. The 10 strains of marine *Synechococcus* spp. examined in this study appear to regulate photosynthetic electron flow at a given temperature by controlling the state transition over a range of irradiances (Fig. 6). All strains were able to cope with high irradiances, and a transition to state 1 was apparent in many of the strains up to  $230 \mu\text{mol quanta m}^{-2} \text{s}^{-1}$  (Fig. 6), suggesting that the PQ pool remained oxidized and PSII excitation pressure was low up to that irradiance. At higher irradiances, the cells were in state 2, and PSII maintains a large light-harvesting cross section that favors oxidation of the PQ pool.

State transitions were also important in regulating electron flow over a range of temperatures, as shown in Figure 7. The  $\Phi_{PSII}$  is a measure of PSII photosynthetic efficiency when the cells are exposed to ambient light. The value represents a balance between the amount of light energy being funneled into the PSII reaction centers and the flow of electrons away from PSII. In low/moderate light, the PBS associates with PSII (state 1) and more light is funneled to the PSII reaction centers compared with that of dark-adapted cells. This suggests that ETC is reduced in the dark because of respiratory electron flow, which triggers a transition to state 2 (PBS affiliated with PSI). Cells in state 1 therefore have a higher PSII fluorescence because of the increased light input from the PBS antenna into PSII compared with dark-adapted cells, even though the number of reaction centers is the same.

In this study, the strongest transition to state 1 was generally observed at the  $100 \mu\text{mol quanta m}^{-2} \text{s}^{-1}$  actinic light level (Fig. 6). For all strains examined in this

study, the effect of state transition on the  $\Phi_{\text{PSII}}$  fluorescence yield at  $100 \mu\text{mol quanta m}^{-2} \text{s}^{-1}$  became more pronounced as the temperature increased (Fig. 7). This effect was independent of  $F_v/F_m$  or the growth rate; the state transition continued to increase even at temperatures above that at which  $F_v/F_m$  and growth had already exceeded their maximum values. For example, the optimal temperatures for  $F_v/F_m$  and doubling time (Td) for strain CCMP837 were  $21^\circ\text{C}$  and  $18^\circ\text{C}$  to  $24^\circ\text{C}$ , respectively (Fig. 5A). The state 1 signal remained strong in this strain up to  $27^\circ\text{C}$  (Fig. 7A), even though  $F_v/F_m$  and growth had both declined to less than 50% of their maximum values at that temperature (Fig. 5A).

The change in yield between  $\Phi_{\text{PSII-100}}$  and  $F_v/F_m$  at a given temperature as shown in Figure 7 reflects the net balance of energy flow into and out of PSII, as described above. At  $100 \mu\text{mol quanta m}^{-2} \text{s}^{-1}$ , some of the PSII reaction centers become reduced as they wait to pass their electrons to downstream acceptors (i.e. excitation pressure increases), and this serves to decrease  $\Phi_{\text{PSII}}$ . The state 2 transition has the opposite effect on the  $\Phi_{\text{PSII}}$ , causing it to increase due to the larger amount of PSII variable fluorescence. Inefficient coupling of the PBS to the photosynthetic apparatus would also contribute to depressed  $\Phi_{\text{PSII}}$  at low temperature (Li et al., 2001) and may result from changes in membrane fluidity (El Bissati et al., 2000) or changes in the oligomeric structure of PSI and PSII at low temperature (Bald et al., 1996). Isolated PBSs, which cannot transfer energy to adjacent molecules, are highly fluorescent (Suter et al., 1984). Increased PBS fluorescence contributes to the dark-adapted steady-state fluorescence,  $F_o$ , and the light-adapted steady-state fluorescence,  $F_s$  (but not  $F_m$  or  $F_m'$ ), and is therefore an alternative mechanism that could lead to lower values of  $\Phi_{\text{PSII}}$  at low temperature, as observed in Figure 7. However, both mechanisms (suppressed transition to state 1 and PBS uncoupling) would serve to decrease PSII excitation pressure at low temperature by limiting energy flow into PSII.

The effect of the state transition is most apparent in pink/orange strains with higher PE content (pigment types 2 and 3; Table I), such as CCMP837 and WH8102, where the  $\Phi_{\text{PSII}}$  actually increases above the  $F_v/F_m$  at  $100 \mu\text{mol quanta m}^{-2} \text{s}^{-1}$ , and the change in yield becomes positive (Fig. 7). To determine if this effect is typical for high-PE *Synechococcus* spp. strains, we grew two additional strains (CCMP838 and CCMP841) at  $15^\circ\text{C}$  and  $27^\circ\text{C}$  to check the generality of the response. CCMP837 and WH8102 are both isolates from the open Atlantic Ocean, whereas CCMP838 and CCMP841 were isolated from more coastal sites. Both of these strains followed the same trend as the other high-PE strains, showing higher values of  $\Phi_{\text{PSII-100}}$  relative to  $F_v/F_m$ . Moreover, the effect was stronger at the higher growth temperature, in keeping with the trends observed in all other strains.

It is important to note that a negative value in Figure 7 does not necessarily indicate lack of state transition in those strains, only that the transition to state 1 did not

increase PSII fluorescence ( $F_m'$ ) strongly enough to mask the effect of increased excitation pressure, which serves to decrease  $\Phi_{\text{PSII}}$ . This was the case for many of the high-PC strains; however, all strains examined in this study showed some degree of state transition based on  $F_m'$  at  $100 \mu\text{mol quanta m}^{-2} \text{s}^{-1}$  being higher than  $F_m$  in the raw fluorescence traces (not shown). A good example of this is represented by the high-PC strain CCMP2606 (Fig. 7I), where the effect of the state transition became more apparent with increasing temperature, eventually causing  $\Phi_{\text{PSII-100}}$  to exceed  $F_v/F_m$  at  $24^\circ\text{C}$  and  $27^\circ\text{C}$ .

#### Response of the *Synechococcus* sp. WH8102 (CCMP2370) Proteome

Based on the photophysiological observations described above, all examined marine *Synechococcus* spp. strains appear to actively regulate photosynthetic electron flow via the state transition, which minimizes PSII excitation pressure under different temperature regimes. This acclimation strategy could manifest as a result of two possible mechanisms. First, it is possible that cells grown at different temperatures retain identical amounts of PBS proteins and that the enhanced transition to state 1 with increasing temperature simply indicates that a larger fraction of these PBSs become associated with PSII under higher temperatures compared with low temperatures. Alternately, the enhanced state transition could be due to greater abundance of PBS proteins at high temperatures. Under the latter scenario, a larger state transition would be observed at high temperature even if the relative proportion of PBS in state 1 versus state 2 was insensitive to temperature.

To investigate the underlying mechanism of the state transition response to temperature in greater detail, we compared the proteome of *Synechococcus* sp. WH8102 grown at  $15^\circ\text{C}$ ,  $18^\circ\text{C}$ , and  $23^\circ\text{C}$  to evaluate the relative abundance of photosynthetic proteins. The abundance of most of the PBS proteins detected either increased or did not change with increasing temperature (Figs. 8 and 9). Prior work has shown that distal parts of the PBS rods are regulated independently from the rest of the complex and become degraded under high light stress (Six et al., 2005). In this study, four proteins associated with APC and PC remained unchanged, while two APC/PC  $\beta$  chain polypeptides increased with temperature. By contrast, all proteins associated with PE I increased with temperature. The PEII linker polypeptide MpeD, a fusion of PE I and II linker polypeptides (Six et al., 2005), was also found to increase with temperature, although no consistent trend was observed for other PE II proteins. Low temperature stress therefore does not appear to favor removal of II rods as does stress from high light. Nevertheless, differential regulation of the PBS components may underlie the variable responses of PBS polypeptides to temperature, and, overall, the trend

was toward an increase in PBS components at higher temperature. The greater capacity for state1 transitions at warmer temperatures could therefore be due in part to the synthesis of more abundant or larger antenna complexes.

The relative abundance of major photosynthetic proteins involved in the ETC, such as constituents of PSI, PSII, and cytochrome b6f complexes, were also observed to increase with temperature (Figs. 8 and 9). This reflects the cell's need to increase photochemistry as cell division increases; the greater abundance of photosynthetic ETC proteins increases the overall photosynthetic electron flux to meet the metabolic demands of the cell for NADPH during rapid growth. The effect of these increases on the redox poise of the ETC is less clear. Along with regulation of state transitions, balanced photosynthetic electron flow is affected by the ratio of PSII and PSI because these complexes control electron flow into and out of the ETC. Global proteome data, such as the data presented in this study, are useful to identify changes in individual proteins across treatments, rather than to calculate protein ratios. However, regardless of whether changes in the PSII/PSI ratio occur in response to temperature, our data suggest that the state transition is important for temperature acclimation and that the activity of PSII and PSI is fine-tuned by the state transition.

The response of ferredoxin and its associated enzymes also showed interesting trends with respect to temperature. The enzymes ferredoxin-NADP reductase, ferredoxin-dependent Glu synthase, and ferredoxin nitrite reductase all increased with increasing temperature (Fig. 8), consistent with the higher demand for reductant and nitrogen metabolism that would occur in rapidly growing cells. However, the abundance of ferredoxin declined as temperature increased. The decline in ferredoxin abundance under high temperature could be in response to the cell prioritizing Fe for other purposes, e.g. Fe is required in large quantities for PSI (12 Fe atoms), cytochrome b6f (six Fe atoms), and PSII (two Fe atoms). Targeted studies to investigate Fe regulation and partitioning among proteins over a range of temperatures would help elucidate the underlying mechanism of this phenomenon.

### The Role of Temperature in *Synechococcus* spp. Biogeography

The PBS is a distinguishing feature of cyanobacteria and is one characteristic that differentiates *Synechococcus* spp. from other types of marine phytoplankton. The ability to tune photosynthesis via movement of the PBS could be one factor contributing to the broader geographic distribution of *Synechococcus* spp. compared with their close relatives *Prochlorococcus* spp., which lack a functional PBS. *Prochlorococcus* spp. do not appear to utilize state transitions via its

chlorophyll *a/b* antenna (Kaňka et al., 2012; A.R. Grossman, unpublished data), and distributions are restricted to tropical waters (45°N to 40°S), where temperature is relatively stable (Partensky et al., 1999a, 1999b; DuRand et al., 2001; Bouman et al., 2006). By contrast, *Synechococcus* spp. are generally less abundant in the tropics but can dominate in subtropical regions with stronger temperature fluctuations. While they do not dominate in polar waters, *Synechococcus* spp. have been found within cooler, high-latitude seas (Huang et al., 2012). Photosynthetic acclimation through the state transition may contribute to *Synechococcus* spp. strains' acclimation to cooler temperatures and allow them to persist throughout colder periods, even as their growth rates slow and they are less numerically abundant. By gaining an early foothold as seasonal temperatures increase in the subtropics, these seed populations would have a competitive advantage over other phytoplankton due to their higher initial abundance. The PBS adaptation may therefore be one factor responsible for the relatively large range of *Synechococcus* spp., by allowing them to persist, albeit at low numbers, in cooler waters.

As a group, the distribution of marine *Synechococcus* spp. is also linked to N availability (Olsen et al., 1990; Partensky et al., 1999a; Paerl et al., 2012), a feature that is likely related to maintenance of the N-rich PBS complex (Wyman et al., 1985; Kana et al., 1992). Under N-replete conditions, the PBS can constitute up to 50% of the protein content of cyanobacterial cells (Cohen-Bazire and Bryant, 1982). Reliance on essential PBS-dependent photoacclimation strategies, a feature that appears to be conserved among *Synechococcus* spp. strains, could therefore be a factor that underlies the high N demands of marine *Synechococcus* spp. The advantage imparted by the ability to acclimate to temperature variability therefore comes with the competitive tradeoff of a potentially higher demand for N per cell due to the PBS. The cellular N quota of *Synechococcus* spp. is roughly twice that of *Prochlorococcus* spp., although their C/N ratio is similar (Bertilsson et al., 2003). Relative to *Prochlorococcus* spp., *Synechococcus* spp. could be at a competitive disadvantage in nutrient-poor, stratified tropical waters with more temperature stability but would be more competitive under the dynamic temperature regimes and N-rich waters found in the subtropics and higher latitudes. The interplay between temperature and N dynamics also fits with the observation that *Synechococcus* spp. in seasonally stratified locations tend to bloom in the spring when the water column transitions from mixed to stratified, such as in the Sargasso Sea (DuRand et al., 2001) and the Red Sea (Lindell and Post, 1995; Mackey et al., 2009; 2011). Such transitions, where SST begins to warm and nitrate is generally still abundant, provide optimal conditions for PBS synthesis and *Synechococcus* spp. growth.

Another observation that arises from this study is the comparison of SST over an annual cycle to the  $T_{opt}$  of each strain (Table I). Some strains grew best at

temperatures above the natural temperature range at their site of origin (e.g. CCMP1632), while others showed the opposite trend (e.g. CCMP837). While it is possible that these different relationships between  $T_{\text{opt}}$  and in situ temperature represent real, natural variability in strain temperature preferences, it is also possible that the strains have adapted to their culture conditions (typically 22°C–26°C) since being isolated. This highlights the importance of using strains that are maintained in a cryopreserved state, which would preserve the original genetic integrity of the strain (LaRoche et al., 2010). While a number of the strains used in this study were obtained from cryopreserved stock, cryopreservation was not routinely followed for strains isolated several decades ago until more recently. However, regardless of strain origin or preservation conditions, a PBS-based photosynthetic strategy appears to be a conserved feature for acclimating to growth at different temperatures among all strains tested in this study.

### Possible Implications from Global Change

Global mean SSTs have already risen above 0.7°C and are projected to rise by approximately 1°C within the next two decades and up to 3°C by the end of the century (IPCC, 2007). Some local and regional areas will of course warm even more. The increased capacity for performing state transitions and synthesizing more photosynthetic proteins could help marine *Synechococcus* spp. as a genus expand further into higher latitudes as SST rises in the future, although other (nonphotosynthetic) acclimation processes will clearly also play a role. Secondary effects from climate warming could compound the direct effect of temperature on *Synechococcus* spp. growth and photosynthesis. By the middle of this century, sea surface warming is expected to lead to the expansion of permanently stratified, low-productivity waters by 4.0% in the northern hemisphere and 9.4% in the southern hemisphere (Sarmiento et al., 2004). These ultraoligotrophic environments receive less input of nutrients such as N and Fe through deep mixing, and surface waters are characterized by vanishingly low levels of these key nutrients (Noble et al., 2012). Acclimation of *Synechococcus* spp. to higher temperatures appears to rely in part on the cell's ability to balance PSII excitation pressure by synthesizing more N-rich pigment proteins and Fe-rich photosynthetic membrane proteins (Fig. 9); however, this strategy would be hampered under prolonged oligotrophic conditions. Future studies should incorporate nutrient limitation over a range of temperatures to help clarify this issue.

### CONCLUSION

The genera *Synechococcus* and *Prochlorococcus* together account for about one-third of total primary

production on Earth (Partensky et al., 1999b) and thus play important roles in Earth's global carbon cycle. Different strains of marine *Synechococcus* spp., adapted to grow under different temperature conditions, have been found at varying abundances at latitudes from the equator to the polar circle (Agusti, 2004; Scanlan et al., 2009; Huang et al., 2012). SSTs are projected to increase by 3°C or more this century, yet very little is known about how *Synechococcus* spp. have adapted to grow at different temperatures in today's ocean or how they might adapt to a future warmer ocean. In this study, we have helped provide a mechanistic understanding of these adaptive capabilities.

A common challenge to all photosynthetic organisms is balancing photosynthetic electron flow with cellular metabolic demands, particularly when acclimating to different temperatures. At suboptimal temperatures where lower growth rates limit downstream electron flow, marine *Synechococcus* spp. prevent PSII excitation pressure by limiting transitions to state 1, thereby decreasing the amount of light energy that PSII receives. At higher temperatures closer to those that drive optimal growth, metabolic processes no longer limit light-driven electron flow, and higher rates of C fixation and N assimilation generate a stronger need for reductant. Under these conditions, a transition to state 1 allows the PBS to channel more energy into PSII, increasing photosynthetic electron flow to match the cell's metabolic needs. In *Synechococcus* sp. WH8102, growth at higher temperature led to increased abundance of photosynthetic proteins, such as those that make up the reaction centers of PSI and the cytochrome b6f complex. The higher abundance of these electron acceptors downstream of PSII, together with the higher demand for reductant resulting from increased growth rates, may serve to facilitate electron flow and maintain PSII reaction centers in an oxidized state, even as the PBS funnels more excitation energy into PSII. The ability of marine *Synechococcus* spp. to regulate photochemistry over a range of temperatures may contribute to the greater distribution of this group relative to *Prochlorococcus* spp., particularly in higher latitude waters, and explain why *Synechococcus* spp. thrive in regions with seasonal temperature variations.

## MATERIALS AND METHODS

### Strains and Growth Conditions

*Synechococcus* spp. strains were procured from the Provasoli-Guillard National Center for Marine Algae and Microbiota. Strains were selected from coastal and oceanic regions throughout the world's oceans (Table I; Fig. 2). Culture medium consisted of a Turk's Island salt water base (Moore et al., 2007) amended with Seawater nitrate medium nutrients (Waterbury et al., 1986) plus 100  $\mu\text{mol L}^{-1}$   $\text{NH}_4^+$  and 10  $\text{nmol L}^{-1}$   $\text{H}_2\text{SeO}_4$  (Keller and Guillard, 1985). The medium was filtered through a 0.2- $\mu\text{m}$  filter and autoclaved to ensure sterility. Dissolved sodium bicarbonate solution was freshly prepared and added to the medium aseptically by passage through a 0.2- $\mu\text{m}$  nitrocellulose membrane to a final concentration of 2  $\text{mmol L}^{-1}$ . Cultures were gently bubbled with 0.2  $\mu\text{m}$  filtered air at all times during the experiment. Culturing

was conducted at 15°C, 18°C, 21°C, 24°C, and 27°C, and cells were allowed to acclimate for at least seven generations prior to sampling. Strains 838 and 841 were only cultured at 15°C and 27°C, and strain PCC 7002 was not cultured at 24°C but was cultured at all other temperatures. Biological replicates were performed for all experiments and each strain/temperature combination was repeated at least three times. The optical density of the culture at 750 nm ( $OD_{750}$ ) was measured on an Ultrospec 3100 Pro spectrophotometer (Amersham Biosciences), and doubling times were determined from these measurements using the equation  $xf = x_i \times 2^{(t/T)}$ , where  $x_f$  is the final  $OD_{750}$  measurement,  $x_i$  is the initial  $OD_{750}$  measurement,  $t$  is the time between measurements, and  $T$  is the doubling time. Strains were grown in semi-continuous batch culture and were diluted every 1 to 3 d, depending on growth rate, to maintain low optical densities and prevent self shading during growth.

Cultures were grown under 35  $\mu\text{mol quanta m}^{-2} \text{s}^{-1}$  continuous light provided by a combination of cool-white and grow light (Sylvania Ecologic) fluorescent bulbs. Temperature was maintained via a thermostat and air conditioning unit for cooling or a radiant space heater for heating. Fans were run continuously to ensure that the temperature was consistent throughout the 1.8- × 1.8-m room, and this was confirmed by three thermometers at different locations within the room. An additional thermometer was placed in a flask of seawater medium that was bubbled identically to the culture flasks, and temperature in the flask was always found to be identical to the ambient air temperature in the room.

### Satellite SST

Weekly SST information was obtained from the National Oceanographic and Atmospheric Administration Earth System Research Laboratory Physical Science Division (<http://www.esrl.noaa.gov/psd/>) for the period of January 1990 through December 2011. Values were extracted from the 1° gridded data set by specifying the latitude and longitude for each strain's site of origin (Table I) using Ferret software. Ferret is a product of the National Oceanic and Atmospheric Administration Pacific Marine Environmental Laboratory.

### PAM Fluorometry

PAM fluorescence was recorded using a WATER-PAM fluorometer with WinControl software (Walz). The actinic light and saturating pulses in the WATER-PAM peak at 660 nm (red light), and the modulated measuring light peaks at 650 nm. Fluorescence was recorded at the exact growth temperature of the culture by housing the WATER-PAM unit inside the temperature-controlled culture room.

The photochemical yield of PSII was determined on 3 mL of culture over a range of irradiances following an 800-ms saturating pulse of light (approximately 6,000  $\mu\text{mol quanta m}^{-2} \text{s}^{-1}$ ). The dark-adapted photochemical efficiency ( $F_v/F_m$ ) was measured on cultures following 3-min dark adaptation in the sample chamber. The light-adapted photochemical efficiency at a given light level ( $\Phi_{PSII}$ ) was measured following 60-s exposure of actinic (background) irradiance of 20, 30, 65, 100, 230, 480, 670, and 1,580  $\mu\text{mol quanta m}^{-2} \text{s}^{-1}$  (Fig. 3). This duration of dark adaptation and actinic light exposure was sufficient to attain steady-state fluorescence before measuring the yield. Between three to eight independent fluorescence traces were obtained for each strain at each growth temperature, for a total of approximately 200 traces analyzed in this study. We note that the strains in this study had contrasting pigment compositions; the PC-rich strains have a larger cross section for red light compared with the PE-rich strains, which have a larger cross section for blue light. Care must therefore be taken in comparing across strains, because for a given actinic (red) light intensity, more of the photons would be absorbed by the PC-rich strains than the PE-rich strains.

Several useful photosynthetic parameters can be derived from fluorescence traces, including  $F_v/F_m$  and  $\Phi_{PSII}$  (see Mackey et al., 2008 for discussion of these parameters). These values are determined from ratios of raw fluorescence levels  $F_v$ ,  $F_m$ ,  $F_s$ , and  $F_m'$  measured over the course of a fluorescence trace, as shown in Figure 3.  $F_0$  and  $F_m$  are measured on dark-adapted samples, while  $F_s$  and  $F_m'$  are determined in the light at each actinic irradiance level. A unique value of  $\Phi_{PSII}$  can therefore be calculated for each actinic irradiance level.  $F_v/F_m$  is calculated as  $(F_m - F_0)/F_m$ , whereas  $\Phi_{PSII}$  is calculated as  $(F_m' - F_0)/F_m'$ . We note that  $F_m$  differs from the maximal fluorescence parameter  $F_M$ . Due to state transitions,  $F_M$  in cyanobacteria is determined using 3-(3,4-dichlorophenyl)-1,1-dimethylurea rather than dark acclimation, as is customary for algae without state transitions (Campbell et al., 1998; Six et al.,

2009). Throughout the text, we refer to the dark-acclimated fluorescence as  $F_m$  to differentiate between these two parameters.

### Global Proteomics of Strain CCMP2370 (WH8102)

Axenic cultures of *Synechococcus* sp. WH8102 were grown in 30  $\mu\text{mol quanta m}^{-2} \text{s}^{-1}$  continuous white light (ProLume F17T8/830 Eco-Shield) as 1-L batch cultures at 15°C, 18°C, and 23°C. Cultures were maintained in SN medium prepared with locally collected natural seawater (salinity, 32 parts per thousand). Cells were harvested in late log phase, pelleted by centrifugation, and stored frozen ( $-80^\circ\text{C}$ ) until processed.

Protein extraction, mass spectrometry, and data processing followed methods described in the supplemental materials section of Saito et al. (2011). Briefly, frozen pellets were resuspended in 100 mM ammonium bicarbonate, sonicated, and centrifuged. Proteins in the supernatants were precipitated at  $-20^\circ\text{C}$  in 100% (v/v) acetone, and the protein pellet was resuspended in 0.1 mL of 6 M urea with 0.1 M ammonium bicarbonate, reduced with 10 mM dithiothreitol, alkylated with 30 mM iodoacetamide, and trypsin digested for 16 h. The tryptic peptides were concentrated onto a peptide cap trap and rinsed with 150  $\mu\text{L}$  0.1% (v/v) formic acid, 5% (v/v) acetonitrile, and 94.9% (v/v) water before gradient elution through a reversed-phase Magic C18 AQ column (0.2 × 150 mm, 3- $\mu\text{m}$  particle size, 200 Å pore size; Michrom Bioresources) on an Advance HPLC system (Michrom Bioresources) at a flow rate of 750 nL  $\text{min}^{-1}$ . The chromatography consisted of a gradient from 5% buffer A to 95% buffer B for 330 min, where A was 0.1% (v/v) formic acid in water and B was 0.1% (v/v) formic acid in acetonitrile. A linear ion trap quadrupole mass spectrometer (Thermo Scientific) was used with an ADVANCE CaptiveSpray source (Michrom Bioresources). The LTQ was set to perform tandem mass spectrometry on the top five ions using data-dependent settings with a dynamic exclusion window of 30 s, and ions were monitored over a range of 400 to 2,000 mass-to-charge ratio. Relative abundance data were normalized to total spectral counts using Scaffold software (Proteome Software) and then log transformed, centered on mean, and normalized in Cluster 3.0. Spectral counts are normalized by multiplying values for all three temperatures for each peptide by a scale factor so that the sum of the squares of the values is 1.0.

### ACKNOWLEDGMENTS

We thank Catherine Lu for laboratory assistance, Gert van Dijken for advice on extracting the gridded SST data, Ken Schneider and Long Cao for discussion of experimental design, and Lanna Cheng, Lillian Govoni, Tracey Riggins, Rebecca Stephen-Smith, and Frederica Valois for helpful discussion on *Synechococcus* spp. strain characteristics and locations of origin.

Received May 22, 2013; accepted August 14, 2013; published August 15, 2013.

### LITERATURE CITED

- Agusti S (2004) Viability and niche segregation of *Prochlorococcus* and *Synechococcus* cells across the Central Atlantic Ocean. *Aquat Microb Ecol* 36: 53–59
- Aro EM, Virgin I, Andersson B (1993) Photoinhibition of photosystem II. Inactivation, protein damage, and turnover. *Biochim Biophys Acta* 1143: 113–134
- Bailey S, Grossman A (2008) Photoprotection in cyanobacteria: regulation of light harvesting. *Photochem Photobiol* 84: 1410–1420
- Bailey S, Melis A, Mackey KR, Cardol P, Finazzi G, van Dijken G, Berg GM, Arrigo K, Shrager J, Grossman A (2008) Alternative photosynthetic electron flow to oxygen in marine *Synechococcus*. *Biochim Biophys Acta* 1777: 269–276
- Bald D, Kruij J, Rogner M (1996) Supramolecular architecture of cyanobacterial thylakoid membranes: how is the phycobilisome connected with the photosystems? *Photosynth Res* 49: 103–118
- Bertilsson S, Berglund O, Karl DM, Chisholm SW (2003) Elemental composition of marine *Prochlorococcus* and *Synechococcus*: implications for the ecological stoichiometry of the sea. *Limnol Oceanogr* 48: 1721–1731
- Brown MV, Schwalbach MS, Hewson I, Fuhrman JA (2005) Coupling 16S-ITS rDNA clone libraries and automated ribosomal intergenic spacer analysis to show marine microbial diversity: development and application to a time series. *Environ Microbiol* 7: 1466–1479
- Bouman HA, Ulloa O, Scanlan DJ, Zwirgmaier K, Li WK, Platt T, Stuart V, Barlow R, Leth O, Clementson L, et al (2006) Oceanographic basis of

- the global surface distribution of *Prochlorococcus* ecotypes. *Science* **312**: 918–921
- Campbell D, Hurry V, Clarke AK, Gustafsson P, Oquist G** (1998) Chlorophyll fluorescence analysis of cyanobacterial photosynthesis and acclimation. *Microbiol Mol Biol Rev* **62**: 667–683
- Cohen-Bazire G, Bryant DA** (1982) Phycobilisomes composition and structure. In NG Carr, BA Whitton, eds, *The Biology of Cyanobacteria*. Blackwell, Oxford, pp 143–190
- DuRand MD, Olsen RJ, Chisholm SW** (2001) Phytoplankton population dynamics at the Bermuda Atlantic Time-series station in the Sargasso Sea. *Deep Sea Res Part II Top Stud Oceanogr* **48**: 1983–2003
- El Bissati K, Delphin E, Murata N, Etienne A, Kirilovsky D** (2000) Photosystem II fluorescence quenching in the cyanobacterium *Synechocystis* PCC 6803: involvement of two different mechanisms. *Biochim Biophys Acta* **1457**: 229–242
- Falk S, Maxwell DP, Laudenbach DE, Huner NPA** (1996) Photosynthetic adjustment to temperature. In NR Baker, ed, *Advances in Photosynthesis and Respiration*, Vol 5. Kluwer, Dordrecht, The Netherlands, pp 367–835
- Fu FX, Warner ME, Zhang YH, Feng YY, Hutchins DA** (2007) Effects of increased temperature and CO<sub>2</sub> on photosynthesis, growth, and elemental ratios in marine *Synechococcus* and *Prochlorococcus* (Cyanobacteria). *J Phycol* **43**: 485–496
- Fuller NJ, Tarran GA, Yallop M, Orcutt KM, Scanlan DJ** (2006) Molecular analysis of picocyanobacterial community structure along an Arabian Sea transect reveals distinct spatial separation of lineages. *Limnol Oceanogr* **51**: 2515–2526
- Gray GR, Ivanov AG, Krol M, Huner NPA** (1998) Adjustment of thylakoid plastoquinone content and photosystem I electron donor pool size in response to growth temperature and growth irradiance in winter rye (*Secale cereale* L.). *Photosynth Res* **56**: 209–221
- Grob C, Ulloa O, Claustre H, Huot Y, Alarcon G, Marie D** (2007) Contribution of picoplankton to the total particulate organic carbon concentration in the eastern South Pacific. *Biogeosciences* **4**: 837–852
- Grossman AR, Schaefer MR, Chiang GG, Collier JL** (1993) The phycobilisome, a light-harvesting complex responsive to environmental conditions. *Microbiol Rev* **57**: 725–749
- Huang S, Wilhelm SW, Harvey HR, Taylor K, Jiao N, Chen F** (2012) Novel lineages of *Prochlorococcus* and *Synechococcus* in the global oceans. *ISME J* **6**: 285–297
- Huner NPA, Maxwell DP, Gray GR, Savitch LV, Krol M, Ivanov AG, Falk S** (1996) Sensing environmental temperature change through imbalances between energy supply and energy consumption: redox state of photosystem II. *Physiol Plant* **98**: 358–364
- IPCC** (2007) Summary for policymakers. In S Solomon, D Qin, M Manning, Z Chen, M Marquis, KB Avearyt, M Tignor, HL Miller, eds, *Climate Change 2007: The Physical Science Basis*. Contribution of Working Group I to the Fourth Assessment Report of the Intergovernmental Panel on Climate Change. Cambridge University Press, New York
- Kaňa R, Kotabová E, Komárek O, Šedivá B, Papageorgiou GC, Govindjee, Prášil O** (2012) The slow S to M fluorescence rise in cyanobacteria is due to a state 2 to state 1 transition. *Biochim Biophys Acta* **1817**: 1237–1247
- Kana TM, Feiweil NL, Flynn LC** (1992) Nitrogen starvation in marine *Synechococcus* strains: clonal differences in phycobiliprotein breakdown and energy coupling. *Mar Ecol Prog Ser* **88**: 75–82
- Keller MD, Guillard RRL** 1985. Factors significant to marine diatom culture. In DM Anderson, AW White, DG Baden, eds, *Toxic Dinoflagellates*. Elsevier, New York, pp 113–116
- Krol M, Maxwell DP, Huner NPA** (1997) Exposure of *Dunaliella salina* to low temperature mimics the high light-induced accumulation of carotenoids and the carotenoid binding protein (Cbr). *Plant Cell Physiol* **38**: 213–216
- LaRoche J, Rost B, Engel A** (2010) Bioassays, batch culture and chemostat experimentation. In U Riebesell, VJ Fabry, L Hansson, JP Gattuso, Guide to Best Practices for Ocean Acidification Research and Data Reporting. Publications Office of the European Union, Luxembourg
- Li Y, Zhang J, Xie J, Zhao J, Jiang L** (2001) Temperature-induced decoupling of phycobilisomes from reaction centers. *Biochim Biophys Acta* **1504**: 229–234
- Lindell D, Post AF** (1995) Ultraphytoplankton succession is triggered by deep winter mixing in the Gulf of Aqaba (Eilat). *Red Sea. Limnol. Oceanogr.* **40**: 1130–1141
- Mackey KRM, Bristow L, Parks DR, Altabet MA, Post AF, Paytan A** (2011) The influence of light on nitrogen cycling and the primary nitrite maximum in a seasonally stratified sea. *Prog Oceanogr* **91**: 545–560
- Mackey KRM, Paytan A, Grossman A, Bailey S** (2008) A photosynthetic strategy for coping in a high light, low nutrient environment. *Limnol Oceanogr* **53**: 900–913
- Mackey KRM, Rivlin T, Grossman AR, Post AF, Paytan A** (2009) Picophytoplankton responses to changing nutrient and light regimes during a bloom. *Mar Biol*
- Maxwell DP, Falk S, Trick CG, Huner NPA** (1994) Growth at low temperature mimics high-light acclimation in *Chlorella vulgaris*. *Plant Physiol* **105**: 535–543
- Mazard S, Ostrowski M, Partensky F, Scanlan DJ** (2012) Multi-locus sequence analysis, taxonomic resolution and biogeography of marine *Synechococcus*. *Environ Microbiol* **14**: 372–386
- Miśkiewicz E, Ivanov AG, Williams JP, Khan MU, Falk S, Huner NPA** (2000) Photosynthetic acclimation of the filamentous cyanobacterium, *Plectonema boryanum* UTEX 485, to temperature and light. *Plant Cell Physiol* **41**: 767–775
- Moore LR, Coe A, Zinser ER, Saito MA, Sullivan MB, Lindell D, Frois-Moniz K, Waterbury J, Chisholm SW** (2007) Culturing the marine cyanobacterium *Prochlorococcus*. *Limnol Oceanogr Methods* **5**: 353–362
- Moore LR, Goericke R, Chisholm SW** (1995) Comparative physiology of *Synechococcus* and *Prochlorococcus*: influence of light and temperature on growth, pigments, fluorescence and absorptive properties. *Mar Ecol Prog Ser* **116**: 259–275
- Mullineaux CW, Tobin MJ, Jones GR** (1997) Mobility of photosynthetic complexes in thylakoid membranes. *Nature* **390**: 421–424
- Noble AE, Lamborg CH, Ohnemus DC, Lam PJ, Goepfert TJ, Measures CI, Frame CH, Casciotti KL, DiTullio GR, Jennings J, et al** (2012) Basin-scale inputs of cobalt, iron, and manganese from the Benguela-Angola front to the South Atlantic Ocean. *Limnol Oceanogr* **57**: 989–1010
- Olsen RJ, Chisholm SW, Zettler ER, Ambrust EV** (1990) Pigment, size, and distribution of *Synechococcus* in the North Atlantic and Pacific Oceans. *Limnol Oceanogr* **35**: 45–58
- Paerl RW, Johnson KS, Welsh RM, Worden AZ, Chavez FP, Zehr JP** (2012) Differential distributions of *Synechococcus* subgroups across the California current system. *Front Microbiol*
- Palenik B, Brahamsha B, Larimer FW, Land M, Hauser L, Chain P, Lamerdin J, Regala W, Allen EE, McCarran J, et al** (2003) The genome of a motile marine *Synechococcus*. *Nature* **424**: 1037–1042
- Palenik B, Ren Q, Dupont CL, Myers GS, Heidelberg JF, Badger JH, Madupu R, Nelson WC, Brinkac LM, Dodson RJ, et al** (2006) Genome sequence of *Synechococcus* CC9311: insights into adaptation to a coastal environment. *Proc Natl Acad Sci USA* **103**: 13555–13559
- Partensky F, Blanchot J, Valout D** (1999a) Differential distribution and ecology of *Prochlorococcus* and *Synechococcus* in oceanic waters: a review. *Bull Inst Oceanogr* **1999** **19**: 457–475
- Partensky F, Hess WR, Valout D** (1999b) *Prochlorococcus*, a marine photosynthetic prokaryote of global significance. *Microbiol Mol Biol Rev* **63**: 106–127
- Saito MA, Bertrand EM, Dutkiewicz S, Bulygin VV, Moran DM, Monteiro FM, Follows MJ, Valois FW, Waterbury JB** (2011) Iron conservation by reduction of metalloenzyme inventories in the marine diazotroph *Crocosphaera watsonii*. *Proc Natl Acad Sci USA* **108**: 2184–2189
- Sarcina M, Tobin MJ, Mullineaux CW** (2001) Diffusion of phycobilisomes on the thylakoid membranes of the cyanobacterium *Synechococcus* 7942. Effects of phycobilisome size, temperature, and membrane lipid composition. *J Biol Chem* **276**: 46830–46834
- Sarmiento JL, Slater R, Barber R, Bopp L, Doney SC, Hirst AC, Kleypas J, Matear R, Mikolajewicz U, Monfray P, et al** (2004) Response of ocean ecosystems to climate warming. *Global Biogeochem Cycles* **18**:
- Scanlan DJ, Ostrowski M, Mazard S, Dufresne A, Garczarek L, Hess WR, Post AF, Hagemann M, Paulsen I, Partensky F** (2009) Ecological genomics of marine picocyanobacteria. *Microbiol Mol Biol Rev* **73**: 249–299
- Six C, Sherrard R, Lionard M, Roy S, Campbell DA** (2009) Photosystem II and pigment dynamics among ecotypes of the green alga *Ostreococcus*. *Plant Physiol* **151**: 379–390
- Six C, Thomas J-C, Garczarek L, Ostrowski M, Dufresne A, Blot N, Scanlan DJ, Partensky F** (2007) Diversity and evolution of phycobilisomes in marine *Synechococcus* spp.: a comparative genomics study. *Genome Biol* **8**: R259

- Six C, Thomas J-C, Thion L, Lemoine Y, Zal F, Partensky F (2005) Two novel phycoerythrin-associated linker proteins in the marine cyanobacterium *Synechococcus* sp. strain WH8102. *J Bacteriol* **187**: 1685–1694
- Suter GW, Mazzola P, Wendler J, Holzwarth AR (1984) Fluorescence decay kinetics in phycobilisomes isolated from the blue-green alga *Synechococcus* 6301. *Biochim Biophys Acta* **766**: 269–276
- Waterbury JB, Watson SW, Valois FW, Franks DG (1986) Biological and ecological characterization of the marine unicellular cyanobacteria *Synechococcus*. *Can Bull Fish Aquat Sci* **214**: 71–120
- Wyman M, Gregory RPF, Carr NG (1985) Novel role for phycoerythrin in a marine cyanobacterium, *Synechococcus* strain DC2. *Science* **230**: 818–820
- Zinser ER, Johnson ZI, Coe A, Karaca E, Veneziano D, Chisholm SW (2007) Influence of light and temperature on *Prochlorococcus* ecotype distributions in the Atlantic Ocean. *Limnol Oceanogr* **52**: 2205–2220
- Zwirgmaier K, Heywood JL, Chamberlain K, Woodward EMS, Zubkov MV, Scanlan DJ (2007) Basin-scale distribution patterns of picocyanobacterial lineages in the Atlantic Ocean. *Environ Microbiol* **9**: 1278–1290
- Zwirgmaier K, Jardillier L, Ostrowski M, Mazard S, Garczarek L, Vault D, Not F, Massana R, Ulloa O, Scanlan DJ (2008) Global phylogeography of marine *Synechococcus* and *Prochlorococcus* reveals a distinct partitioning of lineages among oceanic biomes. *Environ Microbiol* **10**: 147–161